

# Dynamic modulus $E_{kd}$ evaluation by dynamic penetration test

Sebastián López<sup>1\*</sup>, Miguel Benz<sup>2</sup>, Jean Canou<sup>3</sup>, Jean-Claude Dupla<sup>3</sup> and Sebastian Espinoza<sup>4</sup>

<sup>1</sup> Faculty of Engineering, San Sebastián University, Bellavista 7, Recoleta, Chile.

<sup>2</sup> Sol Solution Géotechnique Réseaux, ZA des Portes de Riom Nord, 23 avenue Georges Gershwin, Riom Cedex, 63204, France.

<sup>3</sup> Ecole des Ponts ParisTech, Laboratoire Navier/CERMES, , 6 et 8, av. Blaise Pascal, Cité Descartes, Champs-sur-Marne, 77455 Marne-la-Vallée, CEDEX 2, France.

<sup>4</sup> Pontifical Catholic University of Chile, Macul, Chili.

\* Corresponding author: [sebastian.lopezr@uss.cl](mailto:sebastian.lopezr@uss.cl)

**ABSTRACT.** Dynamic penetration tests *DPT* have been routinely employed in the geotechnical characterization of the subsoil in different types of engineering projects. The evaluation of the results of these tests has been performed considering a limited number of parameters obtained in the field, so the definition of new parameters allows a more accurate evaluation of soil characteristics. The purpose of this paper is to present a methodology for the evaluation of the dynamic modulus ( $E_{kd}$ ) based on the analysis of the dynamic force and velocity signals recorded in each hammer impact. Variable energy *DPT* tests were performed on Fontainebleau *NE34* sand specimens in a  $K_0$  calibration chamber. For each hammer impact on the penetrometer, a decoupling and wave reconstruction method was applied to obtain the force and velocity signals at the cone-soil interface, which are analyzed in the frequency spectrum to obtain the  $E_{kd}$  modulus. The results show that it is possible to evaluate the dynamic modulus at different vertical loading conditions and independent of the impact energy level of the hammer on the penetrometer.

**Keywords:** Dynamic modulus; Dynamic penetration test;  $k_0$  Calibration Chamber; *DPT*.

## 1 Introduction

Dynamic penetration testing *DPT* has been widely employed and has become a useful and indispensable tool in several engineering projects, as it is an alternative to perform a fast and low cost characterization of soil response. In-situ characterization procedures using *DPT* provide valuable data to understand soil behavior and gather the necessary information for the design of geotechnical structures.

The evaluation of dynamic penetration tests has traditionally relied on methodologies such as dynamic driving equations, wave analysis and empirical correlations. However, the complexity of soils and the need for a more accurate assessment has led to the development of more detailed and specific approaches, however, each of the analysis is based on different assumptions and test performance conditions, so the results may not be comparable from one experience to another.

In the context of these differences, the creation of new analysis approaches or the extension of existing ones is necessary, considering elements that allow the comparison between tests or the definition of new parameters based on approaches that can be applied indistinctly to different

equipment under different soil conditions. This article focuses on a specific methodology to evaluate the dynamic modulus ( $E_{kd}$ ) (Tran, Navarrete, & Garcia, 2018; Tran et al., 2019) and effects of soil condition and loading conditions. This parameter allows characterizing the dynamic response of the soil based on the analysis of the frequency spectrum of recorded signals during the test. This methodology is based on the analysis of the dynamic waves of force ( $F(t)$ ) and velocity ( $v(t)$ ) generated by the dynamic impact of a hammer on the striking head of a variable energy dynamic penetrometer and the reconstructed signals at the cone-soil interface (Benz, 2009; Benz, Breul, & Gourvès, 2022; López, 2022).

To capture and measure the dynamic signals, accelerometers and strain gauges located on the penetrometer's striking head are used. These devices measure the signals corresponding to each impact of the hammer throughout the dynamic driving independently of the variability of the impact energy.

The tests were carried out using *NE34* Fontainebleau sand samples, reconstituted by dry deposition in a  $K_0$  calibration chamber, considering a wide range of density indices ( $I_D$ ) and the application of effective vertical loads

( $\sigma'_{v0}$ ) in a range of 10 to 400 *kPa*.

In the following sections of this article, the specific characteristics of the granular material used are specified, along with the operation and characteristics of the dynamic variable energy penetrometer. The methodology for decoupling and reconstruction of the force ( $F(t)$ ) and velocity ( $v(t)$ ) signals that allows obtaining the signals at the cone-soil interface is described. A description of the methodology applied to evaluate the dynamic modulus ( $E_{kd}$ ) and the effects generated on it by the soil state and the applied boundary conditions is presented.

Finally, the results of the laboratory tests are presented and conclusions are drawn regarding the characteristics of  $E_{kd}$  and its sensitivity to the applied soil and boundary conditions.

## 2 Materials and methods

In order to evaluate the dynamic modulus ( $E_{kd}$ ) variable energy *DPT's* were performed on *NE34* Fontainebleau sand specimens. The specimens were reconstituted and tested in a  $K_0$  calibration chamber. Regarding the penetration tests, the tests were performed with a *PANDA 3* variable energy *DPT* equipment. The specifications of the materials, equipment and methods used in the development of this research are presented below.

### 2.1 Granular material

Fontainebleau sand *NE34* is a material composed mainly of silica (98%) with uniform grain size characteristics. It presents a light beige color and its grains exhibit mostly rounded to semi-rounded shapes, in addition to possessing a high resistance to breakage (Benahmed, 2001). For this study, values of  $e_{min} = 0.55$  and  $e_{max} = 0.85$  have been considered for the minimum and maximum void ratios, respectively, which have been obtained by normalized method (AFNOR, 2000). The main geotechnical parameters of this type of sand are detailed in table 1.

**Table 1.** Geotechnical parameters for *NE34* Fontainebleau sands *NE34*.

Parameter	Value
Specific gravity	2,56g/cm <sup>3</sup>
$D_{50}$	0,21 mm
$C_u$	3
$\gamma_{min}$	1,37g/cm <sup>3</sup>
$\gamma_{max}$	1,72g/cm <sup>3</sup>

### 2.2 Calibration chamber $K_0$ .

The  $k_0$  calibration chamber (*CC*) was developed at the Navier laboratory of the Ecole Des Ponts ParisTech (Le, 2014). The *CC* allows the application of geotechnical tests on the reconstituted specimens, as well as to control the saturation and pore pressure conditions inside the mold. This system allows the reconstitution of soil specimens with dimensions of 73 *cm* in height and 55 *cm* in diameter.

The *CC* is composed of two cylinders, a central ring, a base and a top cover, under the top cover and on the reconstituted specimen is installed an extensible rubber membrane, which is driven by hydraulic pressure and which is able to reproduce various soil conditions under different vertical effective stresses ( $\sigma'_{v0}$ ). The assembly is coupled and fixed by means of threaded rods and nuts at the top and bottom 1.

Modifications were made to the top cover system to allow variable energy dynamic penetration testing under controlled vertical load and varying saturation conditions. The modification allowed the application of variable energy during driving and the application of an incremental vertical loading program to capture the soil response under different conditions. (López, 2022)

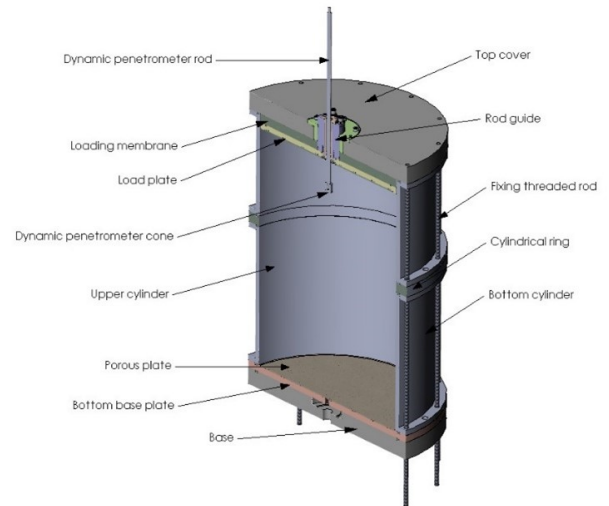


**Figure 1.** Schematic diagram of  $K_0$  calibration chamber.

### 2.3 Variable Energy Dynamic Penetrometer

A *DPT PANDA 3*, dynamic variable energy penetrometer (fig. 2) was used. This equipment developed in France in the 1990's has been widely used around the world in different engineering applications, such as: road infrastructure, airports, railways, mining, among others (Benz et al., 2013; Escobar et al., 2014; Escobar, Benz, Gourvès, Breul,

& Chevalier, 2016; Espinace et al., 2013; López, Dupla, Canou, & Benz, 2021; López & Benz, 2019).

The *DPT* is equipped with acceleration sensors with a measurement range of 20000 *g*, and strain sensors with a measurement range of  $\pm 45$  *kN*. These measurements can be converted into velocity and force measurements by integrating the acceleration signal and applying Hooke's law, respectively. The signals from these sensors are sent to a Central Data Acquisition Unit (*UCA*) (French: *Unité d'Acquisition de Données*), via a cable connection. In this unit, data are processed, stored and, additionally, transmitted wirelessly to a mobile device for viewing and interpretation. To complement the dynamic measurements, the *UCA* is equipped with a displacement sensor connected to the striking head (fig. 2).

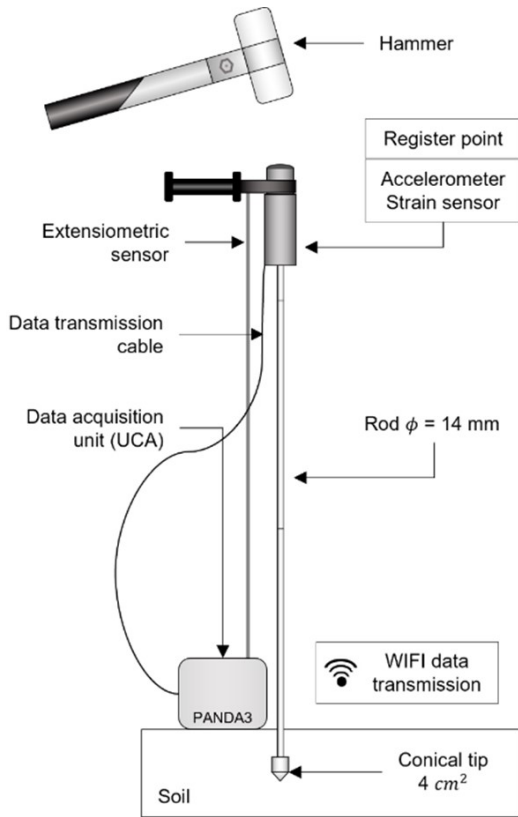


**Figure 2.** Dynamic Variable Energy Penetrometer *DPT* general scheme.

To extend the analysis of measurements during the tests, the dynamic force ( $F(f)$ ) and velocity ( $v(t)$ ) signals of each impact (fig. 3) can be analyzed in the time and frequency domain. This feature allows taking advantage of the evaluation of alternative geotechnical parameters, such as: the mechanical impedance of the soil ( $Z_s$ ), the wave velocity in the soil ( $C_p$ ) through the application of the polar shock method (Benz et al., 2022), the dynamic elastic

modulus ( $E_{kd}$ ), dynamic tip resistance, among others (Tran et al., 2018, 2019; Benz et al., 2022; López, 2022).

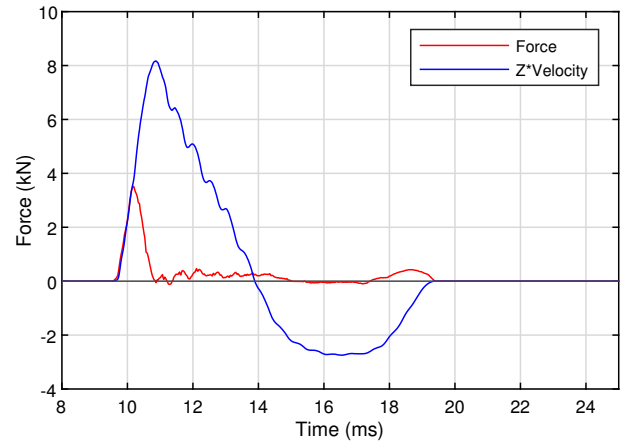


**Figure 3.** Dynamic force and velocity signals measured at the striking head.

The dynamic signals analysis at each impact of the hammer is carried out by applying the wave theory. Due to the morphological characteristics of the penetrometer, it is possible to analyze the problem from a one-dimensional approach (eq. 1). This approach is based on the assumption of a constant wave propagation velocity ( $C_r$ ), the elastic behavior of rods, homogeneous cross section, as well as on the consideration of negligible external lateral forces applied on the rods.

$$\frac{\delta^2 y}{\delta x^2} = \frac{1}{c^2} \frac{\delta^2 y}{\delta t^2} \quad (1)$$

The one-dimensional wave equation can be analyzed by means of the D'Alembert solution. This solution proposes the superposition of two waves propagating in opposite directions: an incident wave ( $u_i$ ), and a reflected wave ( $u_r$ ) (eq. 2).

$$u(x, t) = u_i(x - ct) + u_r(x + ct) \quad (2)$$

Measurement of  $u_i$  and  $u_r$  at a known point ( $x_a$ ) of the device allows determination of the strain ( $\epsilon(x, t)$ ), stresses ( $\sigma(x, t)$ ), velocities ( $v(x, t)$ ), and displacement ( $u(x, t)$ ) at any point ( $x_n$ ) along the penetrometer by applying a decoupling and wave reconstruction procedure (Benz, 2009; Benz et al., 2022; López, 2022).

### 2.3.1 Decoupling and wave reconstruction

The wave generated by the hammer impact on the striking head travels through the penetrometer body in a descending and ascending way, producing a wave superposition phenomenon, so it is necessary to apply a decoupling

method that allows the visualization of the waves (Casem, Fourney, & Chang, 2003; Jung, Park, & sik Park, 2006; Lundberg & Henchoz, 1977; Benz, 2009; Benz et al., 2022; López, 2022) (figure 4).

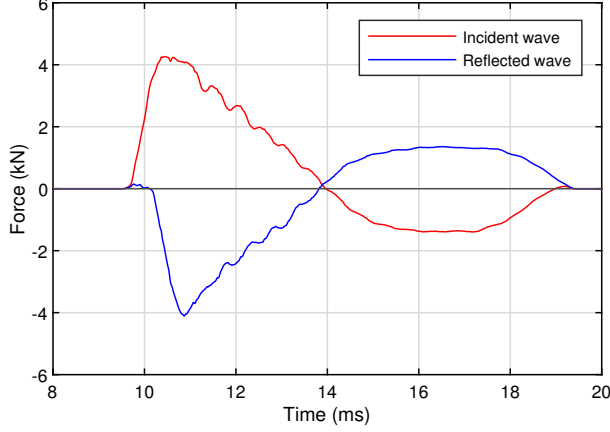


**Figure 4.** Incident  $u_i$  and reflected  $u_r$  decoupling wave.

In the case of the PANDA 3 penetrometer, it was determined that the most appropriate method is the one presented by Casem et al (2003) (Benz, 2009; Benz et al., 2022). The proposed method allows obtaining the incident ( $u_i$ ) and reflected ( $u_r$ ) wave signals at a known measurement point ( $x_a$ ) inside the penetrometer using deformation measurements ( $varepsilon_a(t)$ ) and velocity ( $v_a(t)$ ) (eq. 3 and eq. 4).

$$\varepsilon_d(x - ct) = \frac{1}{2} \left[ \varepsilon_A(t) - \frac{v_a(t)}{c} \right] \quad (3)$$

$$\varepsilon_r(x + ct) = \frac{1}{2} \left[ \varepsilon_A(t) + \frac{v_a(t)}{c} \right] \quad (4)$$

If the force and velocity signals are available at a penetrometer known point, the wave propagation medium is homogeneous and the lateral friction effects are considered negligible, it is possible to reconstruct the signals at any point along the penetrometer (eq. 5 and eq. 6) (Carlsson, Sundin, & Lundberg, 1990; Karlsson, Lundberg, & Sundin, 1989). The above characteristics are not completely fulfilled, however, it is possible to apply an iterative process of decoupling and reconstruction of the dynamic signals at each impedance change point. In the case of the effects associated with the lateral friction of rods, it is indicated that the energy losses associated with this interaction can be neglected since they are less than 1.5% (Odebrecht, Schnaid, Maia, & de Paula, 2005; Palacios, 1977).

$$F_N(t) = \frac{1}{2} [F_{N-1}(t + \Delta t_{n-(n-1)}) + F_{N-1}(t - \Delta t_{n-(n-1)})] \\ + \frac{1}{2Z_n} [v_{N-1}(t + \Delta t_{n-(n-1)}) - v_{N-1}(t - \Delta t_{n-(n-1)})] \quad (5)$$

$$v_N(t) = \frac{1}{2} [v_{N-1}(t + \Delta t_{n-(n-1)}) + v_{N-1}(t - \Delta t_{n-(n-1)})] \\ + \frac{1}{2Z_r} [F_{N-1}(t + \Delta t_{n-(n-1)}) - F_{N-1}(t - \Delta t_{n-(n-1)})] \quad (6)$$

The force ( $F_t(t)$ ) and velocity ( $v_t(t)$ ) signals reconstructed at the soil-cone interface (figure 5 and 6), allow the construction of a dynamic load-displacement curve which represents the response of the soil to the dynamic load imposed by the cone (Benz, 2009; Benz et al., 2022). It is also possible to analyze the signals in the frequency spectrum, from which the dynamic modulus ( $E_{kd}$ ) is calculated (Tran et al., 2018, 2019; López, 2022).

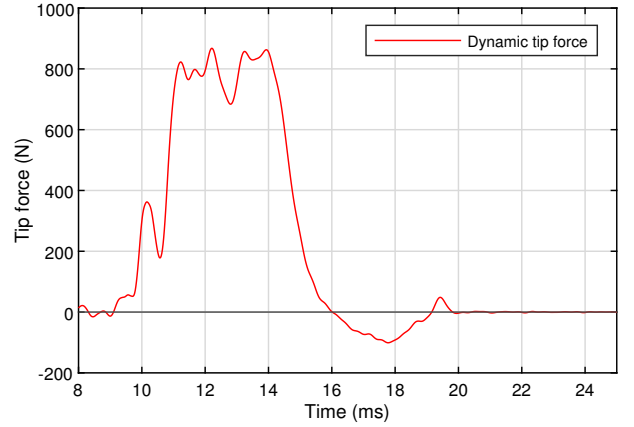


**Figure 5.** Señal de fuerza  $F_t(t)$  reconstruida en la interfaz cono-suelo.

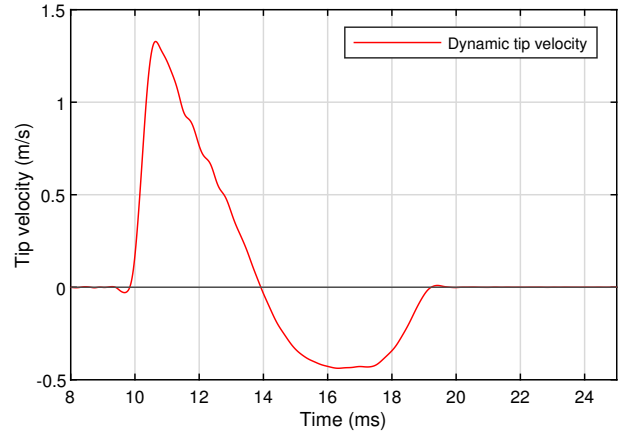


**Figure 6.** Señal de velocidad  $v_t(t)$  reconstruida en la interfaz cono-suelo.

## 2.4 Evaluation of the dynamic modulus $E_{kd}$

The soil response can be analyzed on the basis of the frequency spectrum. The shock wave caused by the hammer impact on the penetrometer produces vibration phenomena both in the equipment and in the soil that can be analyzed in the frequency domain by applying transfer functions (eq. 7 and 8) to the force and velocity signals both at the striking head and at the cone-soil interface. This feature provides the possibility to determine the properties of the penetrometer-soil system and to analyze how it responds to the hammer impact on the equipment's by means of parameters such as the dynamic modulus ( $E_{kd}$ ), which is a dynamic parameter representing the elastic response of the soil in the frequency domain.

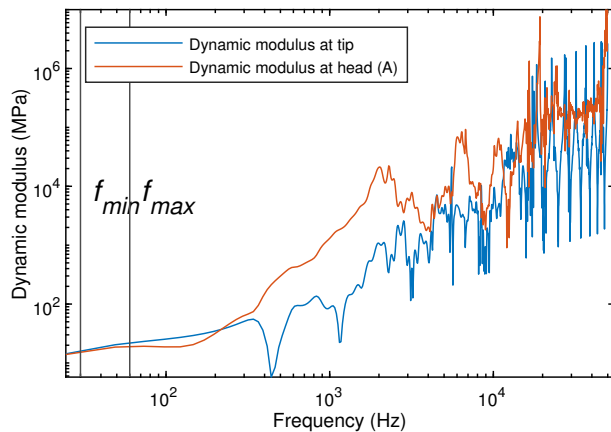
The dynamic modulus can be determined by employing the raw dynamic signals for each hammer impact on the striking head. First, it is possible to obtain the dynamic stiffness ( $k_d(f)$ ) by the ratio between the force signal ( $F(f)$ ) and displacement signal ( $S(f)$ ) (eq. 9); then, considering the conical tip as a circular plate embedded in a semi-infinite elastic medium, it is possible to apply the Boussinesq approach (eq. 10) to calculate the dynamic modulus ( $E_{kd}$ ) as a function of frequency ( $f$ ) (fig. 7).

$$F(t) \longleftrightarrow F(f) = FFT[F(t)] \quad (7)$$

$$v(t) \longleftrightarrow v(f) = FFT[v(t)] \quad (8)$$

$$k_d = \frac{F(f)}{S(f)} \quad (9)$$

$$E_{kd} = \frac{1 - \nu^2}{d_p} k_d \quad (10)$$



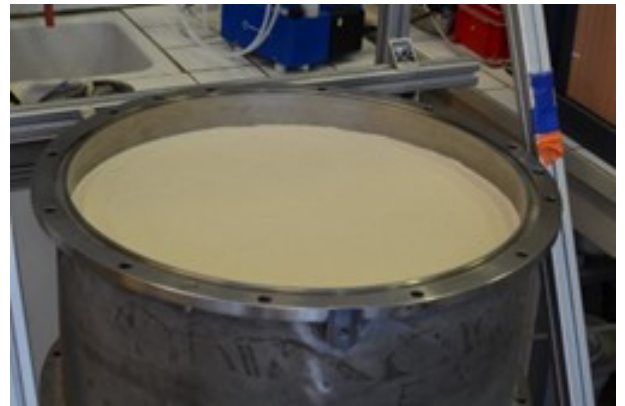
**Figure 7.**  $E_{kd}$  dynamic modulus spectra at the striking head and soil-cone interface.

Fig. 7 shows the dynamic modulus spectra computed for the signals obtained at the striking head and at the soil-cone interface by applying the decoupling and reconstruction signal method. From these spectra, it is possible to determine the frequency range for which both spectra are linearly proportional. The range of proportionality depends on the soil compaction state and the nature of the soil. The higher the stiffness of the soil, the wider the frequency range in which the proportionality of the spectra is maintained.

Considering the dependence of the range of proportionality of the spectra on the soil state, it is necessary to define maximum ( $f_{max}$ ) and minimum ( $f_{min}$ ) frequency limits, for which a maximum dynamic modulus ( $E_{kdmax}$ ) and a minimum ( $E_{kdmin}$ ) are defined. The  $f_{min}$  is associated with the measurement capabilities of the test device and is set at a frequency of 24 Hz. The  $f_{max}$  is defined as the divergence point of the dynamic modulus ( $E_{kd}(f)$ ) (fig. 7). Determining the values of  $f_{max}$  and  $f_{min}$  defines the average pre-frequency value, which in turn defines the value of the dynamic modulus ( $E_{kd}$ ).

## 2.5 Experimental procedure

To calculate the dynamic modulus ( $E_{kd}$ ) and establish the relationship between this parameter and the soil state, 4 dynamic penetration tests were performed in a  $k_0$  CC. Each test was performed on specimens reconstituted by dry and layered deposition to ensure a state of homogeneous compactness and a density index ( $I_D$ ) (or relative density) of 0.3, 0.5, 0.7 and 0.9 for each specimen, respectively (fig. 8).



**Figure 8.** Reconstituted sand specimen.

To obtain the dynamic signals, a variable energy DPT test was performed at the center of each of the reconstituted specimens. In each test, acceleration and deformation signals were measured for each dynamic impact performed on the striking head. From the measured signals the particu-



lar velocity was obtained by applying the integration of the acceleration and force by applying Hooke's law with the strain signal.



**Figure 9.** Dynamic penetrometer installed and dynamic driving over the specimen.

For the measurements of each impact, the decoupling and reconstruction method was applied to determine the force and velocity signals at the soil-core interface. The signals were analyzed in the frequency domain to establish the relationship representing the dynamic modulus ( $E_{kd}(f)$ ).

Each test was performed by applying an effective vertical stress program ( $\sigma'_{v0}$ ) in levels of 10, 25, 50, 75, 75, 100, 200, 300 and 400 *kPa* to capture the soil response under different loading conditions.

To avoid problems associated with boundary effects, impacts generated after exceeding 10 centimeters of depth from the top surface of the specimen were included in the analysis, and those generated at a distance of less than 10 centimeters from the base of the specimen were excluded. In addition, the verticality of the driving was ensured by means of leveling measurements.

### 3 Experimental results

The dynamic modulus ( $E_{kd}$ ) was obtained for each hammer impact on the 4 sand specimens tested and for each

vertical effective stress level. A penetrogram presenting the dynamic modulus ( $E_{kd}$ ) for each impact on a reconstituted specimen at an  $I_D$  of 0.70 is shown in Fig. 10. In the penetrogram, it is possible to observe that the higher the vertical stress applied to the specimen, the higher the magnitude of  $E_{kd}$ . This result was obtained in each of the tests performed.

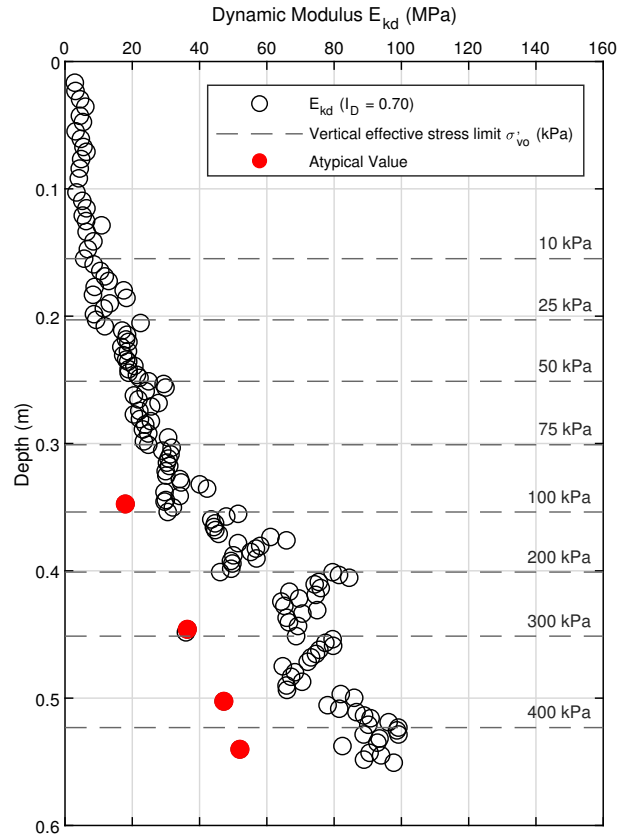


**Figure 10.** Dynamic modulus  $E_{kd} - I_D$  relationship as a function of vertical effective stress  $\sigma'_{v0}$ .

The occurrence of outlier points was observed (fig. 10). The occurrence of this phenomenon is related to the eccentricity of the hammer impacts that generate lateral deformations and interaction with elements of the calibration chamber; however, the exclusion of these points does not affect the evaluation of the dynamic modulus. To obtain a representative parameter at different vertical loading conditions, the average value of the  $E_{kd}$  in each vertical effective stress interval was obtained.

The results obtained from the tests made it possible to obtain the dynamic modulus ( $E_{kd}$ ) for each hammer impact and consequently the construction of relationships between the dynamic modulus ( $E_{kd}$ ), the soil density index ( $I_D$ ), and the vertical effective stress applied ( $\sigma'_{v0}$ ) on the reconstituted specimen in the CC.

The relationship between  $E_{kd}$  and  $I_D$  can be presented as a logarithmic relationship (11) (López, 2022), whose general function is defined by a  $\alpha$  factor and a  $\beta$  factor (eq. 11). These factors are unique for each soil type and its state; however, normalization factors can be applied to make the results comparable with test results on other soil types under a different range of vertical loading conditions.

$$I_d = \alpha \ln(E_{kd}) + \beta \quad (11)$$

Figure 11 shows the relationship established between the density index ( $I_D$ ) and the dynamic modulus ( $E_{kd}$ ) for vertical stresses of 50, 100 and 200  $kPa$ . It is possible to establish that the curves fitting the relationship shift to the right the higher the effective vertical stress (Higher vertical effective stress implies a higher  $E_{kd}$  magnitude.). In the case of the density index, it is observed that the denser the state of the soil, the greater the magnitude of the dynamic modulus ( $E_{kd}$ ), establishing greater differences, the higher the  $I_D$ .

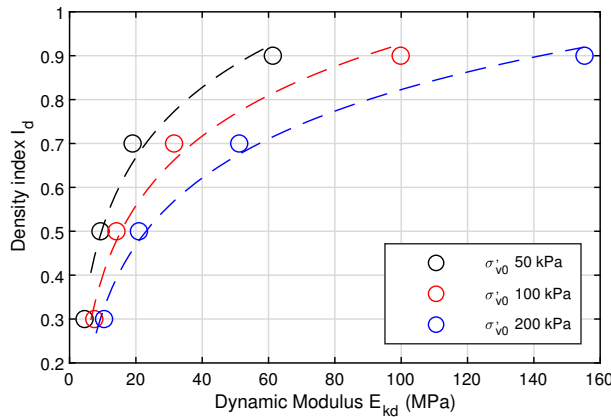


Figure 11.  $E_{kd}$ - $I_d$  relationships for  $\sigma_{v0}$  of 50, 100 and 200  $kPa$ .

A summary of the  $\alpha$  and  $\beta$  parameters that model the relationship between soil density state and dynamic modulus for all ranges of effective vertical stress applied to the specimens is presented in table 2; in addition, the  $r^2$  ratio coefficient is presented. From the relationships and their coefficient  $r^2$ , it can be observed the high level of accuracy of the correlation, demonstrated by values of  $r^2$  greater than 0.95.

Table 2.  $\alpha$  and  $\beta$  parameter para relaciones  $E_{kd}$ - $I_d$  relationships.

$\sigma_{v0}$	$\alpha$	$\beta$	$r^2$
10	0,2143	0,2005	0,9524
25	0,2078	0,1531	0,9903
50	0,2306	-0,0228	0,9835
75	0,2241	-0,0702	0,9598
100	0,2288	-0,1271	0,982
200	0,2198	-0,1894	0,9896
300	0,2178	-0,2391	0,9883
400	0,2697	-0,5196	0,9741

## 4 Conclusions

A methodology for the dynamic modulus ( $E_{kd}$ ) evaluation has been presented by performing variable energy dynamic penetration tests on NE34 Fontainebleau sand specimens reconstituted in a  $k_0$  calibration chamber at different density states and subjected to different vertical effective levels. Obtaining this parameter allows to extend the analysis of the soil response subjected to dynamic penetration generated by the application of variable energy driving.

The results of the application of the  $E_{kd}$  evaluation methodology based on the processing of dynamic force and velocity signals at the soil-cone interface obtained by an iterative process of decoupling and wave reconstruction were presented.

It is possible to conclude that the applied methodology allows the evaluation of  $E_{kd}$  for each hammer impact on the penetrometer to describe parametrically the soil response soil subjected to a dynamic load at a known depth.

With respect to the soil density state, it is concluded that the magnitude of  $E_{kd}$  increases as  $I_D$  increases; likewise, the greater the magnitude of the vertical effective load, the greater the magnitude of  $E_{kd}$ .

Although there is a long history in the use of dynamic penetrometers, the application of variable energy and the application of the technique of decoupling and reconstruction of force and velocity signals under these conditions has begun to become widespread since the 1990s. This is why the analysis of the test results tending to the evaluation of the soil response through new parameters such as  $E_{kd}$  allows generating an extension in the possibility of using this type of geotechnical equipment and allows extending its application; however, many of the elements associated with the analysis methods are still under development, so it is concluded that there is a need for a continuous improvement of the technique and an extension of the engineering practice using variable energy penetrometers.

## Acknowledgements

Aknowledgments to french FUI project EMeRG3r (Elaboration des Méthodes de Reconnaissance Géotechnique de 3ème Génération, 2018-2022)” for partial funding of the project.

## References

- AFNOR. (2000). *Nfp94-059 soils : investigation and testing - determination of minimal and maximal density of cohesionless soils*. Association française de Normalisation.
- Benahmed, N. (2001). *Comportement mécanique d'un sable sous cisaillement monotone et cyclique : application aux phénomènes de liquéfaction et de mobilité y cylique* (Unpublished doctoral dissertation).
- Benz, M. (2009). *Mesures dynamiques lors du battage du penetrometre panda 2* (phdthesis).
- Benz, M., Breul, P., & Gourvès, R. (2022, 2). Application of wave equation theory to improve dynamic cone penetration test for shallow soil characterisation. *Journal of Rock Mechanics and Geotechnical Engineering*, 14, 289-302. doi: 10.1016/j.jrmge.2021.07.004
- Benz, M., Escobar, E., Gourvès, R., Haddani, Y., Breul, P., & Bacconnet, C. (2013). Mesures dynamiques lors du battage pénétrométrique – détermination de la courbe charge-enfoncement dynamique en pointe. In *18th international conférence on soil mechanics and geotechnical engineering* (p. 499-502).
- Carlsson, J., Sundin, K. G., & Lundberg, B. (1990). A method for determination of in-hole dynamic force-penetration data from two-point strain measurement on a percussive drill rod. *International Journal of Rock Mechanics and Mining Sciences and*, 27, 553-558. doi: 10.1016/0148-9062(90)91006-S
- Casem, D. T., Fourny, W., & Chang, P. (2003). Wave separation in viscoelastic pressure bars using single-point measurements of strain and velocity. *Polymer Testing*, 22, 155-164. doi: /10.1016/S0142-9418(02)00064-8
- Escobar, E., Benz, M., Gourvès, R., Breul, P., & Chevalier, B. (2016). Dynamic characterization of the supporting layers in railway tracks using the dynamic penetrometer panda 3®. In *International conference on transportation geotechnics ictg* (Vol. 143, p. 1024-1033). Elsevier B.V. doi: 10.1016/j.proeng.2016.06.099
- Escobar, E., Benz, M. A., Haddani, Y., Lamas, F., Calon, N., & Aguiar, S. C. D. (2014). Reconnaissance dynamique des sites ferroviaires a l'aide du penetrometre panda 3®. In *Journées nationales de géotechnique et de géologie de l'ingénieur*.
- Espinace, R., Villavicencio, G., Palma, J., Breul, P., Bacconnet, C., Benz, M., & Gourvès, R. (2013). Stability of chilean's tailings dams with the panda® penetrometer. experiences of the last 10th. In *18th international conference on soil mechanics and geotechnical engineering* (p. 519-522).
- Jung, B., Park, Y., & sik Park, Y. (2006). Longitudinal acceleration wave decomposition in time domain with single point axial strain and acceleration measurements longitudinal acceleration wave decomposition in time domain with single point axial strain and acceleration measurements. In *8th international conference on motion and vibration control*.
- Karlsson, L. G., Lundberg, B., & Sundin, K. G. (1989). Experimental study of a percussive process for rock fragmentation. *International Journal of Rock Mechanics and Mining Sciences and*, 26, 45-50. doi: 10.1016/0148-9062(89)90524-X
- Le, V. (2014). *Étude sur modèle physique du renforcement des sols par colonnes en soil-mix: application aux plates-formes ferroviaires* (Unpublished doctoral dissertation).
- Lundberg, B., & Henchoz, A. (1977). Analysis of elastic waves from two-point strain measurement. *Experimental Mechanics*, 17, 213-218. doi: 10.1007/bf02324491
- López, S. (2022). *Development of a method to evaluate the risk of liquefaction of sands from a dynamic penetrometer test* (phdthesis).
- López, S., & Benz, M. (2019). Comparación de los ensayos de penetrómetro de cono dinámico de energía variable panda® ensayo de placa de carga estática y dinámica. In *Xvi pan-american conference on soil mechanics and geotechnical engineering*. doi: 10.3233/STAL190206
- López, S., Benz, M., & Moustan, P. (2019). Comparación de los ensayos de penetración de cono dinámico (dcp) y penetrómetro de cono dinámico de energía variable panda®. In *Xvi pan-american conference on soil mechanics and geotechnical engineering*. doi: 10.3233/STAL190206
- López, S., Benz, M., Navarro, J., & Zamora, D. (2018). Control geotécnico de obras viales mediante penetrómetro dinámico ligero de energía variable panda 2. In *X congreso chileno de geotecnia*.
- López, S., Canou, J., Dupla, J.-C., & Benz, M. (2021). Development of a liquefaction risk assessment methodology using an instrumented lightweight dynamic penetrometer: calibration chamber tests. In *6th in-*



- ternational conference on geotechnical and geophysical site.*
- López, S., Canou, J., Dupla, J. C., & Navarrete, M. B. (2020). Penetrometre dynamique et indice de densite des sables. application a l'évaluation du risque de liquefaction des massifs sableux. In *Journées nationales de géotechnique et de géologie de l'ingénieur.*
- López, S., Dupla, J.-C., Canou, J., & Benz, M. (2021). Evaluation of soil liquefaction resistance with variable energy dynamic penetration test, panda®: state of the art. In *6th international conference on geotechnical and geophysical site.*
- Odebrecht, E., Schnaid, F., Maia, M., & de Paula, G. (2005). Energy efficiency for standard penetration tests. *Journal of Geotechnical and Geoenvironmental Engineering*, 131, 1252-1263. doi: 10.1061/(ASCE)1090-0241(2005)131:10(1252)
- Palacios, A. (1977). *The theory and measurement of energy transfer during standard penetration test sampling* (Unpublished doctoral dissertation).
- Tran, Q. A., Navarrete, M. A. B., Breul, P., Chevalier, B., Moustan, P., TRAN, Q. A., & NAVARRETE, M. A. B. (2019). Soil dynamic stiffness and wave velocity measurement through dynamic cone penetrometer and wave analysis. In *Xvi congreso panamericano de mecánica de suelos e ingeniería geotécnica* (p. 401-408). doi: 10.3233/STAL190064
- Tran, Q. A., Navarrete, M. B., & Garcia, M. G. (2018). Determination of soil's dynamic stiffness trough panda 3® and spectrum signal processing. In *Journées nationales de géotechnique et de géologie de l'ingénieur* (p. 1-9).